Published in Optics Letters 44, issue 4, 3470-3473, 2019
which should be used for any reference to this work

10 kHz linewidth mid-infrared quantum cascade laser by stabilization to an optical delay line

Atif Shehzad,* Pierre Brochard, Renaud Matthey, Thomas Südmeyer, and Stéphane Schilt

Laboratoire Temps-Fréquence, Institut de Physique, Université de Neuchâtel, CH-2000 Neuchâtel, Switzerland
**Corresponding author: atif.shehzad@unine.ch*

We present a mid-infrared quantum cascade laser (QCL) with a sub-10 kHz full width at half-maximum linewidth (at 1 s integration time) achieved by stabilization to a free-space optical delay line. The linear range in the center of a fringe detected at the output of an imbalanced Mach–Zehnder interferometer implemented with a short free-space pathlength difference of only 1 m is used as a frequency dis-criminator to detect the frequency fluctuations of the QCL. Feedback is applied to the QCL current to lock the laser fre-quency to the delay line. The application of this method in the mid-infrared is reported for the first time, to the best of our knowledge. By implementing it in a simple self-homodyne configuration, we have been able to reduce the frequency noise power spectral density of the QCL by almost 40 dB below 10 kHz Fourier frequency, leading to a line-width reduction by a factor of almost 60 compared to the free-running laser. The present limits of the setup are assessed and discussed.

Distributed-feedback (DFB) quantum cascade lasers (QCLs) offer a unique combination of high output power, single-mode emission, and continuous spectral tunability that make them the most widely used type of continuous-wave laser sources in the mid-infrared (MIR) molecular fingerprint spectral region for gas-phase spectroscopy and trace gas sensing applications. The intrinsic or Schawlow-Townes linewidth [1] of DFB-QCLs that results from the laser white frequency noise can be as low as a few hundred hertz [2]. However, excess electrical flicker noise in the semiconductor structure that induces internal temperature fluctuations of the laser active region [3,4], as well as the technical noise that may arise from the current driver [5], lead to a broadening of the observed QCL emission linewidth (full width at half-maximum [FWHM]) to the megahertz level, typically, for integration times of milliseconds to hundreds of millisecond [2,3,6–8]. This is most often sufficient for gas sensing and many molecular spectroscopy applications, but more advanced applications that aim at controlling molecular degrees of freedom, for example, to test fundamental symmetries, or to measure fundamental constants and their possible time variation [9], require QCLs with a lower frequency noise and, thus, a narrower linewidth.

Different fairly simple approaches have been implemented to reduce the frequency noise of QCLs, e.g., by using the voltage noise detected between the QCL terminals as an error signal in a stabilization loop [10,11], but these methods resulted in a modest reduction of the frequency noise power spectral density (FN-PSD) by typically one order of magnitude. More sophisticated setups involved stabilization to a reference optical cavity. However, high-finesse cavities are much less developed in the MIR than in the near-infrared (NIR) range, where lasers stabilized down to the sub-hertz level are routinely used [12–15] today in optical clocks or for ultra-low noise microwave generation. Therefore, only a few works of direct laser stabilization to a MIR high-finesse cavity have been reported. M.S. Taubman and co-workers measured a heterodyne beat note with a linewidth of a few hertz only between two cavity-stabilized QCLs at 8.5 μm [16], but the measurement did not constitute an absolute assessment of the linewidth of these lasers, as the two cavities were locked to each other with a bandwidth of 6 kHz. Fasci *et al.* reported a 1 ms linewidth of less than 4 kHz for an 8.6 μm QCL locked to a high-finesse V-shaped cavity by optical feedback [17]. However, the most stable and low-frequency noise lasers in this spectral region have been achieved by phase-locking a QCL to a cavity-stabilized NIR laser through a nonlinear process using a frequency comb, leading to fairly complex setups [9,18].

An alternative method to an optical cavity enabling a significant reduction of the frequency noise of a laser was demonstrated in the NIR with the use of a much simpler setup based on an optical delay line [19–21]. The interference fringes occurring in an imbalanced Michelson or Mach–Zehnder interferometer act as a frequency discriminator that converts frequency fluctuations of the laser into intensity fluctuations, which are detected by a photodiode at the interferometer output. In the interferometer, part of the light is delayed in one path by propagating through a time delay before being recombined with the other part of the light that propagates through a much shorter path. The magnitude of the discrimination factor (in V/Hz) is approximately given by $2\pi\tau V_{\mathrm{pk}}$, where τ is the imbalanced interferometer time delay, and V_{pk} is the amplitude of the error signal [19]. The most standard configuration makes use of a frequency-shifter acousto-optic modulator (AOM) in one arm to produce a self-heterodyne beat signal at the interferometer output. This beat signal is demodulated at the

shifting frequency to stabilize the laser emission frequency to the delay line, by applying a feedback signal either directly to the laser driver, or to another AOM, resulting in a high feedback locking bandwidth. Thus, high laser noise reduction can be achieved, and a resulting linewidth at the sub-hertz level has been demonstrated in the NIR using a 500 m fiber length in a Michelson interferometer [21].

As the resulting frequency discrimination factor scales linearly with the pathlength difference between the two interferometer arms, long delay lines lead to a high discriminator factor and, thus, to a high-frequency noise sensitivity. In the NIR, long delays of hundreds of meters to a few kilometers are easily achievable using low-loss single-mode optical fibers. Hence, very low FN-PSD was demonstrated for a 1.5 μm laser stabilized to a kilometer-scale fiber delay, comparable to the residual noise achieved by stabilization to an ultra-low expansion (ULE) high-finesse optical cavity in a large range of Fourier frequencies [20]. Only at low offset frequencies (typically below 100 Hz), the laser stabilized to the delay line was affected by higher frequency noise and drift resulting from acoustic/mechanical noise and thermal drift of the interferometer, as compared to a ULE cavity that is usually better protected against such disturbances by being mounted in a more advanced protective enclosure.

In this Letter, we demonstrate a significant frequency noise reduction achieved for the first time, to the best of our knowledge, for a MIR QCL by stabilization to an optical delay line. However, AOMs are much less common in the MIR range than in the NIR and, furthermore, require a high radio-frequency power resulting in an elevated power dissipation and the need for a water cooling that can induce excess noise in the interferometer. Therefore, a self-heterodyne configuration as used with NIR lasers is not convenient at MIR wavelengths. Hence, our proof-of-principle demonstration reported here is based on a simpler self-homodyne scheme that does not need an AOM. Consequently, this scheme is much more sensitive to $1/f$ flicker noise arising from laser intensity noise and detector noise that may limit the achieved frequency noise of the stabilized laser. Furthermore, the poor availability of low-loss single-mode optical fibers in the MIR prevents the use of a fiber delay line. Hence, we restricted the experimental setup to a short free-space pathlength difference of around 1 m acting as a frequency-to-amplitude noise converter in this first proof-of-principle demonstration.

With this scheme, we nevertheless achieved a QCL FN-PSD reduction by almost 40 dB over a large range of Fourier frequencies and a narrowing of the corresponding linewidth below 10 kHz at 1 s integration time, as compared to almost 500 kHz for the free-running laser. A scheme of the experimental setup is shown in Fig. 1. A DFB-QCL emitting at ~7.8 μm (from Alpes Lasers, Switzerland) and driven by a homemade low-noise current source is coupled to a Mach–Zehnder interferometer with a pathlength difference of ~90 cm. The laser is operated at a temperature of 20°C and an average current of ~435 mA located approximately in the middle of its operation range at this temperature. At this operation point, its current-tuning coefficient was assessed to be −0.29 GHz/mA. This value was spectroscopically obtained from the position of several N_2O absorption lines observed in a large current scan through a low-pressure gas cell and their comparison to the Hitran database [22]. A second-order fit of the QCL frequency versus current was performed to extract the tuning coefficient at

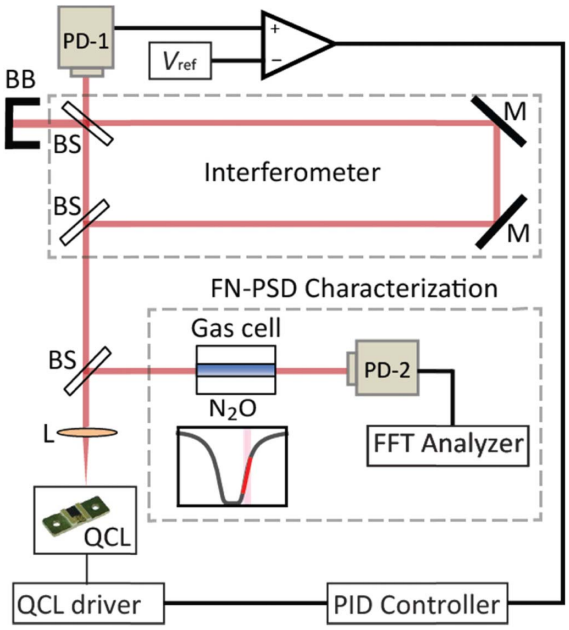

Fig. 1. Experimental setup for QCL frequency noise reduction using a delay line; L, lens; BS, beam splitter; M, mirror; PD, photodetector; BB, beam blocker, PID, proportional-integral-derivative servo controller; FFT, fast Fourier transform. The linear range of an N_2O transition in a gas cell (red part of the absorption line) is used to measure the frequency noise of the laser with a frequency-to-voltage conversion factor of 27.9 V/GHz.

the operating point. The beat signal at the output of the interferometer is detected with a Mercury-Cadmium-Telluride photodiode (Vigo Systems, model PVMI-4TE-8) and is compared to a stable reference voltage V_{ref} to generate an error signal for the laser frequency stabilization. The interference fringes observed when scanning the QCL frequency (via a current scan) are displayed in Fig. 2. A high contrast of the interference of about 90% is achieved here with an optimized alignment of the interferometer, which is important to get a high discrimination factor that lowers the noise floor of the setup, as discussed later. The measured slope $D_{\mathrm{fringe}} = 7.9$ V/GHz in the center of a fringe is in good agreement with the calculated value $2\pi\tau V_{pk} = 8.3$ V/GHz assessed from the applied pathlength difference of ~88 cm, and the observed fringe amplitude of 0.45 V. The reference voltage is adjusted so that the zero-crossing point of the resulting error signal lies in the middle of a fringe, in the linear range. A proportional-integral-derivative (PID) servo-controller (Vescent D2-125) amplifies the error signal and produces a feedback signal that is applied to the current driver of the QCL. A feedback bandwidth larger than 100 kHz is typically needed to achieve a substantial reduction of the QCL frequency noise and linewidth according to the crossing point of the FN-PSD of the free-running laser with the β-separation line [23]. The impact of acoustic and mechanical noise on the interferometer was reduced by enclosing the whole experimental setup in a closed wooden box whose walls are covered by a foam layer. Some foam was additionally placed underneath the optical breadboard of the interferometer.

Before the interferometer, a beam splitter directs part of the laser output beam through a 10-cm-long sealed gas cell filled with a low pressure (2 mbar) of pure N_2O that is followed by a

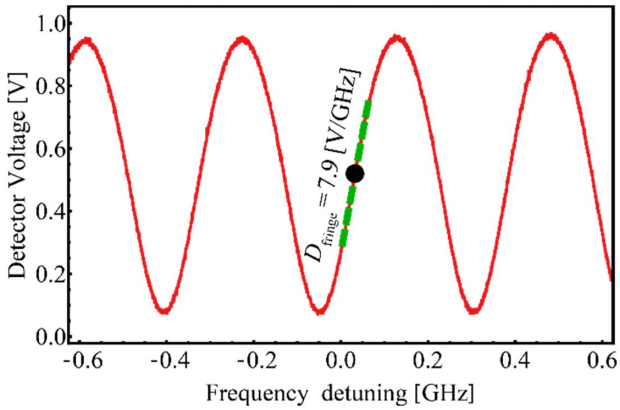

Fig. 2. Interference fringes detected at the output of the interferometer when scanning the QCL current. The locking point indicated by a black dot is located in the linear range of a fringe with a slope D_{fringe}. The frequency axis of the graph was obtained using the measured tuning coefficient of the QCL of –0.29 GHz/mA.

photodiode. This setup is used to independently characterize the frequency noise of the laser (absolute out-of-loop measurement). The laser is tuned to the flank of a strong N_2O absorption line at 1276.4 cm^{-1}, which acts as a frequency discriminator with a typical conversion coefficient $D_{\text{gas}} = 27.9$ V/GHz measured in the setup (see Fig. 1). The voltage noise of the detector signal is measured with a fast Fourier transform (FFT) analyzer (Rhode-Schwarz FSWP-26) and is converted into laser frequency noise using the measured frequency discriminator, for both the free-running and locked laser. The frequency noise of the free-running QCL was also assessed from the error signal using the slope of the fringe (D_{fringe}) around the locking point displayed in Fig. 2 for a cross-check. The two distinct measurements of the FN-PSD of the free-running QCL displayed in Fig. 3 are in good agreement, which proves their proper scaling with the discriminators slopes D_{gas} or D_{fringe}, respectively.

The results of the stabilization to the delay line show a significant noise reduction (by almost 40 dB) at Fourier frequencies lower than 10 kHz. A locking bandwidth slightly lower than 400 kHz is assessed from the servo bump in the FN-PSD. However, the locked laser is affected by a fairly large $1/f$ noise at low frequencies. This is a consequence of the self-homodyne scheme implemented here, as the beat signal detected around DC is sensitive to $1/f$ noise originating from different sources such as laser intensity noise and detector noise. The narrow noise peaks occurring at frequencies of 50 Hz and odd harmonics in the spectrum of the locked laser are of an electronic origin, while the series of broader noise features below 1 kHz result from acoustic and mechanical noise in the interferometer, which is transferred to the laser by the feedback.

In order to identify the present limitation in the setup, different noise floors have been measured (see Fig. 4). The noise floor of the characterization setup (frequency discriminator from the gas cell and associated detector) was assessed by recording the combination of the voltage noise of the detector (PD-2) and of the laser intensity noise without the reference gas cell. The measured voltage noise floor was converted into an equivalent frequency noise floor by scaling with the measured frequency discriminator slope D_{gas}. One notices that the spectroscopic frequency noise characterization setup used here does not constitute a limitation at the presently achieved noise level of the QCL. Hence, this simple spectroscopic setup is suitable to characterize the frequency noise of a laser with a linewidth around or closely below 10 kHz (provided that its intensity noise is not too large). However, there is only little margin between the measured FN-PSD of the locked QCL and the noise floor of the characterization setup, so that a steeper frequency discriminator (e.g., obtained from a sub-Doppler transition) would be needed to characterize the noise of a narrower linewidth laser, e.g., at the level of a few kilohertz or below.

The achieved frequency noise of the stabilized QCL matches the system noise floor obtained when blocking one beam in the interferometer, which sets the limit corresponding to the detector noise and laser intensity noise. The measured noise was converted into an equivalent FN-PSD by scaling with the interferometer frequency discrimination factor $D_{\text{fringe}} = 7.9$ V/GHz (see Fig. 2). The associated $1/f$ noise currently limits the achieved frequency noise of the locked QCL at Fourier frequencies in the range of around 20 Hz to 1 kHz. At lower frequencies, the drift of the interferometer is likely

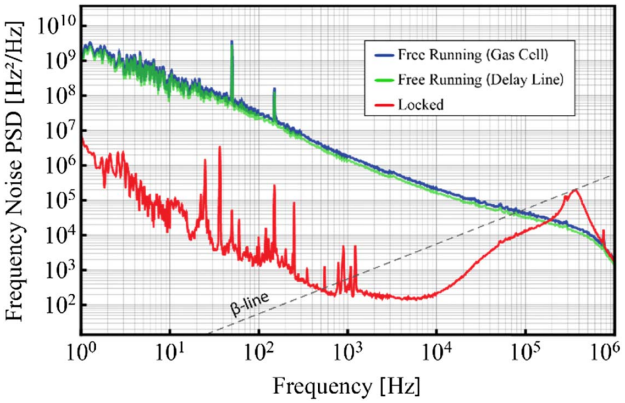

Fig. 3. Frequency noise PSD of the QCL in free-running (blue and green curves measured in two different ways) and locked (red) modes. The servo bump of the locked laser indicates a locking bandwidth of ~400 kHz. The gray dashed line corresponds to the β-separation line used to calculate the corresponding laser linewidth [23].

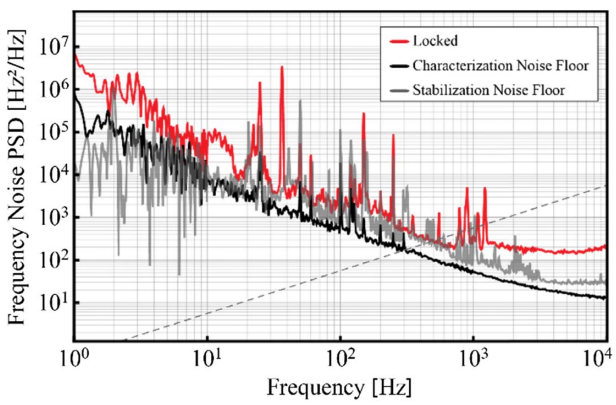

Fig. 4. Comparison of the frequency noise PSD of the locked laser with the noise floors originating from the characterization and stabilization parts of the experimental setup.

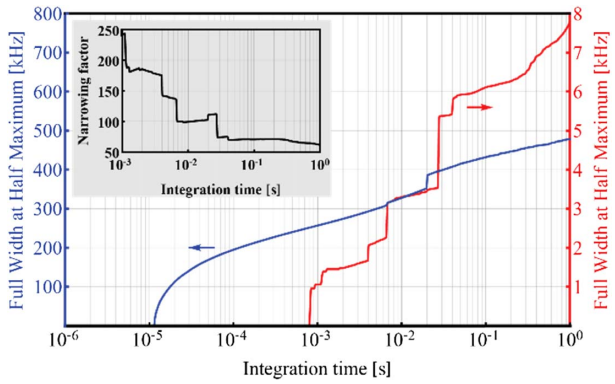

Fig. 5. FWHM linewidth of the QCL calculated from the frequency noise spectrum based on the β-separation line approximation [23] as a function of the integration time (inverse of the lower cutoff frequency for the FN-PSD integration) in a free-running regime (blue) and for the QCL stabilized to the delay line (red). Inset: linewidth narrowing factor as a function of the integration time.

responsible for the observed laser frequency noise that is no longer limited by the detector or intensity noise.

The laser linewidth estimated from the measured FN-PSD using the β-separation line approximation [23] is 7.8 kHz at 1 s integration time, which is 60 times narrower than the linewidth of the free-running laser (Fig. 5). This reduction factor is even larger than 100 at shorter integration times of 10 ms and below. The achieved linewidth narrowing is much higher than with other simple approaches previously reported for frequency noise reduction in QCLs [10,11], while being obtained with a fairly simple setup consisting of only of a few standard optical components (two gold-coated mirrors and two polarization-independent beam splitters in the interferometer). This simple arrangement does not involve any vacuum chamber, temperature stabilization of the setup, or active anti-vibration platform.

In conclusion, we have reported, to the best of our knowledge, the first proof-of-principle demonstration of QCL frequency noise reduction using a free-space delay line. The achieved results are presently limited by the implemented self-homodyne scheme and by the fact that a fairly short imbalance pathlength (less than 1 m) is used in this experiment. The next steps to improve the stabilization will consist on one hand of increasing the pathlength difference to enhance the sensitivity to the laser frequency noise and decrease the stabilization noise floor, which can be achieved for instance with the use of a multipass cell to keep the setup compact. On the other hand, we will implement an absolute lock of the delay line to a molecular transition to combine the linewidth reduction brought by the stabilization to the delay line with the absolute frequency stability of the molecular reference.

Funding. Swiss National Science Foundation (SNSF) (200020_178864); European Space Agency (ESA).

REFERENCES

1. A. L. Schawlow and C. H. Townes, Phys. Rev. **112**, 1940 (1958).
2. S. Bartalini, S. Borri, P. Cancio, A. Castrillo, I. Galli, G. Giusfredi, D. Mazzotti, L. Gianfrani, and P. De Natale, Phys. Rev. Lett. **104**, 083904 (2010).
3. L. Tombez, S. Schilt, J. Di Francesco, P. Thomann, and D. Hofstetter, Opt. Express **20**, 6851 (2012).
4. S. Schilt, L. Tombez, C. Tardy, A. Bismuto, S. Blaser, R. Maulini, R. Terazzi, M. Rochat, and T. Südmeyer, Appl. Phys. B **119**, 189 (2015).
5. L. Tombez, S. Schilt, J. Francesco, T. Führer, B. Rein, T. Walther, G. Domenico, D. Hofstetter, and P. Thomann, Appl. Phys. B **109**, 407 (2012).
6. L. Tombez, J. Di Francesco, S. Schilt, G. Di Domenico, J. Faist, P. Thomann, and D. Hofstetter, Opt. Lett. **36**, 3109 (2011).
7. S. Bartalini, S. Borri, I. Galli, G. Giusfredi, D. Mazzotti, T. Edamura, N. Akikusa, M. Yamanishi, and P. De Natale, Opt. Express **19**, 17996 (2011).
8. S. Schilt, L. Tombez, G. D. Domenico, and D. Hofstetter, in *The Wonder of Nanotechnology: Quantum Optoelectronic Devices and Applications* (SPIE, 2013).
9. B. Argence, B. Chanteau, O. Lopez, D. Nicolodi, M. Abgrall, C. Chardonnet, C. Daussy, B. Darquié, Y. Le Coq, and A. Amy-Klein, Nat. Photonics **9**, 456 (2015).
10. L. Tombez, S. Schilt, D. Hofstetter, and T. Südmeyer, Opt. Lett. **38**, 5079 (2013).
11. I. Sergachev, R. Maulini, A. Bismuto, S. Blaser, T. Gresch, Y. Bidaux, A. Müller, S. Schilt, and T. Südmeyer, Opt. Lett. **39**, 6411 (2014).
12. J. Alnis, A. Matveev, N. Kolachevsky, Th. Udem, and T. W. Hänsch, Phys. Rev. A **77**, 053809 (2008).
13. K. Numata, A. Kemery, and J. Camp, Phys. Rev. Lett. **93**, 250602 (2004).
14. T. Kessler, C. Hagemann, C. Grebing, T. Legero, U. Sterr, F. Riehle, M. J. Martin, L. Chen, and J. Ye, Nat. Photonics **6**, 687 (2012).
15. D. G. Matei, T. Legero, S. Häfner, C. Grebing, R. Weyrich, W. Zhang, L. Sonderhouse, J. M. Robinson, J. Ye, F. Riehle, and U. Sterr, Phys. Rev. Lett. **118**, 263202 (2017).
16. M. S. Taubman, T. L. Myers, B. D. Cannon, R. M. Williams, F. Capasso, C. Gmachl, D. L. Sivco, and A. Y. Cho, Opt. Lett. **27**, 2164 (2002).
17. E. Fasci, N. Coluccelli, M. Cassinerio, A. Gambetta, L. Hilico, L. Gianfrani, P. Laporta, A. Castrillo, and G. Galzerano, Opt. Lett. **39**, 4946 (2014).
18. M. G. Hansen, E. Magoulakis, Q.-F. Chen, I. Ernsting, and S. Schiller, Opt. Lett. **40**, 2289 (2015).
19. B. S. Sheard, M. B. Gray, and D. E. McClelland, Appl. Opt. **45**, 8491 (2006).
20. F. Kéfélian, H. Jiang, P. Lemonde, and G. Santarelli, Opt. Lett. **34**, 914 (2009).
21. J. Dong, Y. Hu, J. Huang, M. Ye, Q. Qu, T. Li, and L. Liu, Appl. Opt. **54**, 1152 (2015).
22. L. S. Rothman, I. E. Gordon, Y. Babikov, A. Barbe, D. C. Benner, P. F. Bernath, M. Birk, L. Bizzocchi, V. Boudon, L. R. Brown, A. Campargue, K. Chance, E. A. Cohen, L. H. Coudert, V. M. Devi, B. Drouin, A. Fayt, J.-M. Flaud, R. R. Gamache, J. J. Harrison, J.-M. Hartmann, C. Hill, J. Hodges, D. Jacquemart, A. Jolly, J. Lamouroux, R. J. Le Roy, G. Li, D. A. Long, O. M. Lyulin, C. J. Mackie, S. Massie, S. Mikhailenko, H. S. P. Müller, O. V. Naumenko, A. V. Nikitin, J. Orphal, V. Perevalov, A. Perrin, E. R. Polovtseva, C. Richard, M. A. H. Smith, E. Starikova, K. Sung, S. Tashkun, J. Tennyson, G. Toon, Vl, G. Tyuterev, and G. Wagner, J. Quant. Spectrosc. Radiat. Transf. **130**, 4 (2013).
23. G. Di Domenico, S. Schilt, and P. Thomann, Appl. Opt. **49**, 4801 (2010).